Hindawi
Wireless Communications and Mobile Computing
Volume 2023, Article ID 9805253, 1 page
https://doi.org/10.1155/2023/9805253

Retraction

Retracted: Oblique Crack Propagation of Brittle Rock under Uniaxial Compression and Its Influencing Factors

Wireless Communications and Mobile Computing

Received 13 September 2023; Accepted 13 September 2023; Published 14 September 2023

This article has been retracted by Hindawi following an investigation undertaken by the publisher [1]. This investigation has uncovered evidence of one or more of the following indicators of systematic manipulation of the publication process:

(1) Discrepancies in scope
(2) Discrepancies in the description of the research reported
(3) Discrepancies between the availability of data and the research described
(4) Inappropriate citations
(5) Incoherent, meaningless and/or irrelevant content included in the article
(6) Peer-review manipulation

The presence of these indicators undermines our confidence in the integrity of the article's content and we cannot, therefore, vouch for its reliability. Please note that this notice is intended solely to alert readers that the content of this article is unreliable. We have not investigated whether authors were aware of or involved in the systematic manipulation of the publication process.

Wiley and Hindawi regrets that the usual quality checks did not identify these issues before publication and have since put additional measures in place to safeguard research integrity.

We wish to credit our own Research Integrity and Research Publishing teams and anonymous and named external researchers and research integrity experts for contributing to this investigation.

The corresponding author, as the representative of all authors, has been given the opportunity to register their agreement or disagreement to this retraction. We have kept a record of any response received.

References

[1] H. Wang and H. Tian, "Oblique Crack Propagation of Brittle Rock under Uniaxial Compression and Its Influencing Factors," *Wireless Communications and Mobile Computing*, vol. 2022, Article ID 1951885, 7 pages, 2022.

Hindawi
Wireless Communications and Mobile Computing
Volume 2022, Article ID 1951885, 7 pages
https://doi.org/10.1155/2022/1951885

Research Article

Oblique Crack Propagation of Brittle Rock under Uniaxial Compression and Its Influencing Factors

Han Wang[1] **and Haoyuan Tian**[2]

[1]*School of Civil Engineering and Construction, Hubei University of Technology, Wuhan Hubei 430068, China*
[2]*Wuhan Surveying-Geotechnical Research Institute Co., Ltd. of MCC Shenzhen Branch, Wuhan Hubei 430080, China*

Correspondence should be addressed to Han Wang; 101910614@hbut.edu.cn

Received 5 May 2022; Revised 23 May 2022; Accepted 25 May 2022; Published 28 June 2022

Academic Editor: Kalidoss Rajakani

With the development of infrastructure in China, the slope rock mass is affected by external forces such as roads. Tunnel excavation will cause a series of engineering problems, which are essentially caused by the instability caused by the propagation of internal cracks in the rock mass. At the same time, in practical engineering, the rock mass is formed through long-term geological structure, and its internal cracks have a variety of properties. Based on granite samples as the research object, two different angles of sample shapes, cylindrical and circular, are prefabricated. The uniaxial compression test is studied to analyze the law of inclined crack propagation in rock under uniaxial compression. Combined with the theory of fracture mechanics, the influence mechanism of crack inclination and sample shape on crack propagation in rock mass is discussed. The test results show that under uniaxial compression, the stress-strain curves of granite samples can be divided into four stages: compaction, elasticity, plasticity, and residual deformation. For the cylindrical sample, the crack initiation occurs at the tip. The compressive strength of the sample decreases with the increase in the prefabricated crack angle, and the crack initiation angle increases with the increase in the prefabricated crack angle. The fracture of the sample changes from shear slip failure to split shear failure of the penetrating rock mass with the increase in the crack angle. For the disk sample, the crack initiation location gradually increases from the tip to the middle with the increase in the crack angle, and the crack initiation angle increases with the increase in the crack angle. The peak load of the sample decreases first and then increases with the increase in the crack angle and is the minimum at 60°. The fracture mode of the sample is mainly tensile failure. When the crack dip angle is between 30° and 60°, the tensile and shear composite failure of the sample occurs, and the influence mechanism of crack dip angle and sample shape on the crack propagation path is analyzed. The research results have important theoretical significance for engineering design, construction, and stability maintenance.

1. Introduction

With the rapid development of economy and society, people put forward higher requirements for living and environmental conditions. In order to solve the needs of human life, China has rapidly started large-scale geotechnical engineering such as highway, railway, hydropower station, nuclear power plant, mine, and oil and gas exploitation, which is closely related to the foundation, slope, and other problems. In the face of complex geotechnical engineering problems, rock mass instability caused by crack propagation has become a major safety problem affecting engineering construction at home and abroad. Crack propagation in rock mass may lead to partial or overall instability of engineering, tilting of surface buildings or delivery rooms, highway subsidence, tunnel collapse, and other accidents, which seriously threaten the safety of life and property of the country and people. Therefore, the study of crack propagation law and its influencing factors in rock mass has important guiding significance for the safety of geotechnical engineering construction [1–3].

The propagation of cracks in rock mass has always been a key research topic in geotechnical engineering, and there have been fruitful research results. Some researchers have proposed that the failure of rock mass is mainly due to crack

propagation and connection, which leads to the decline of bearing capacity, and the bearing capacity will decline rapidly after the crack propagation in the sample. For engineering rock mass, it is impossible to conduct crack propagation experiments on site, so most scholars carry out indoor experiments to study the crack propagation mechanism of samples under different loading conditions. Based on laboratory simulation tests, some researchers have carried out crack propagation studies of samples with different loading rates and crack angles. It is concluded that the loading rate can change the crack propagation mode, and the crack angle affects the crack initiation position of samples [4–8]. Some researchers carried out uniaxial compression experiments on samples with natural cracks and divided the crack propagation into two stages: microscopic particle damage and macroscopic crack propagation. Some researchers studied the influence of the shape and number of cracks on the mechanical properties of samples by prefabricating cracks with different properties and numbers. Some scholars have studied the influence of different filling materials in the sample cracks on the compressive strength of the sample and obtained the influence of filling materials on the strength and deformation behavior of the sample under uniaxial compression. Some scholars have studied the effect of prefabricated double cracks on the mechanical properties of specimens and concluded that the crack initiation and propagation are related to the crack angle, and the crack initiation usually starts from the tip. Crack extension within some researchers who studied the sample form by means of a prefabricated crack compressive shear test was carried out on the marble; it is concluded that in the single crack sample, the sample with a crack inclination of 30° produces two symmetrical airfoil cracks propagating along the principal stress direction, and the sample with an inclination of 45° produces airfoil cracks and secondary cracks [9–13]. With the renewal of experimental instruments, some researchers observed the crystal dislocation phenomenon of granodiorite under stress through an electron microscope and scanning electron microscope and concluded that the grain interface slip and microcrack diffusion creep occurred in granite quartz crystal, indicating that obvious plastic deformation occurred in the rock, accompanied by dislocation slip and other behaviors [14].

A lot of laboratory experiments have been carried out on crack propagation in rock mass, but the mechanism and influencing factors of crack propagation have not been systematically studied. In this paper, the propagation law of prefabricated cracks in granite samples is studied. The cylindrical and disk-shaped samples with different inclination cracks are prefabricated, and the uniaxial compression test is carried out to analyze the propagation law and failure mode of inclined cracks in the samples under uniaxial compression and to study the influence mechanism of crack inclination and sample shape on the propagation of internal cracks in rocks, so as to provide reference for engineering design. Provide theoretical guidance and data support for construction [15–18].

2. Materials and Methods

2.1. Sample Preparation. Cores were collected from the Xinjiang region, and drilled cores at different depths (50 m, 100 m, 150 m, and 200 m) were obtained by drilling. Cores are mainly medium-fine grained speck-bearing biotite granodiorite. Detailed records of core collection are shown in Table 1.

The diameter of drilled cores retrieved from the site was 63 mm. In order to meet the requirements of samples, cores were processed by core machines, cutting machines, and grinding machines to prepare cylindrical and disc samples. For the cylindrical sample (Figure 1(a)), the diameter of the cylinder is 51 ± 3 mm, the height to diameter ratio is 2.0~2.5, the unevenness deviation of the two ends of the sample is within ±0.05 mm, and the cross section and the sample axis should be vertical and the error is within ±0.25° according to the "Standard for Engineering Rock Mass Test Method" GB/T 50266-99. For the disk sample (Figure 1(b)), the diameter of the disk is 55 ± 3 mm and the height is 20 ± 1 mm. The requirements for the unflatness deviation of the two ends of the sample and the error of the section perpendicular to the axis of the sample are the same as those of the cylindrical sample.

Due to the high hardness of granite, in order to make cracks on the sample, the high-pressure water knife cutting method was used to prefabricate 25 mm long and 3 mm wide cracks, and keep the crack center at the geometric center of the rock sample, and the included angles between the prefabricated cracks and the test loading direction were 0°, 15°, 30°, 45°, 60°, 75°, and 90°, respectively.

2.2. Experimental Scheme and Method. After the sample is prepared, the test scheme is designed. According to crack angle and no crack, the cylindrical samples were divided into 8 groups, wo groups of atr each depth, 3 in each group, with a total of 24. The loading direction of the sample was drawn on the surface of the disk sample, and the angle between the loading and the crack was recorded. The samples were divided into 8 groups with and without cracks, wo groups of atr each depth, 3 in each group, with a total of 24 samples.

The RMT-150C rock mechanics testing machine (Figure 2) was used to carry out a uniaxial compression test on the cylindrical sample to obtain the compressive strength, axial strain, and other parameters of the sample as well as the crack morphology after failure. The specific processes are as follows:

(1) The sample was put into the sleeve and in contact with the longitudinal and circumferential strain pointers, respectively. The sample was preloaded to make the experiment fully in contact with the pointers

(2) The axial strain control was adopted during the experiment, and the strain rate was 10^{-5} ~10^{-6} s^{-1}

(3) During the test, input the diameter D and height H of the sample and relevant parameters of the sensor to the computer. The system automatically records the force and stress during the test (calculated automatically by the force value and the sample area), strain, displacement, and other parameters, and arrange the required parameter values after the test

Table 1: Drilling core acquisition records.

The serial number	Sample number	Sampling location		The length of the sample (m)	The sample name
		Back to the time	Start point-end point (m)		
1	TH-1	1	49.23~53.53	4.3	Medium-fine grained patchy biotite granodiorite
2	TH-2	2	98.50~102.42	3.92	Medium-fine grained patchy biotite granodiorite
3	TH-3	3	148.11~151.32	3.21	Medium-fine grained patchy biotite granodiorite+fine grained granitic dikes
4	TH-4	4	200.17~204.21	4.04	Medium-fine grained patchy biotite granodiorite

(a) Cylindrical specimen (b) Disc specimen

Figure 1: Sample diagram.

Figure 2: RMT-150C rock mechanics testing machine.

(4) After the sample reaches the compressive strength, the system will stop automatically when it reaches the protection value. If the sample reaches the peak strength, there is still residual strength, and the stress slowly decreases but the strain still develops. When the stress drops to close to zero, a manual stop is performed. At this time, the stress-strain curve of the sample is recorded, and the crack morphology of the sample after failure is photographed (Figure 3(a)).

Uniaxial compression tests were carried out on cylindrical specimens using the RMT-150C rock mechanics testing machine to obtain peak stress and peak strain of specimens and crack morphology after failure. The specific process is as follows: the disk specimen is placed in a special fixture, and then, the disk specimen is placed according to the angle of the crack and the loading direction; the testing machine is started, so that the sample is in contact with the pointer surface, and then, the preloading makes the specimen fully in contact with the loading surface, so as to fix the disk angle. At the end of preloading, the system loading was zeroed, and a 150 kN pressure profile was used to load at a loading rate of 0.2 MPa/s. The test was stopped after the main fracture of the sample was loaded and the specimen was obviously no longer bearing pressure. Peak stress and strain were recorded, and crack morphology of the damaged sample was photographed (Figure 3(b)).

3. Results

3.1. Experimental Results of Cylindrical Specimens. For cylindrical samples, the axial strain and compressive strength of each sample were obtained through the uniaxial compression test, as shown in Table 2. According to Table 2, the changes of compressive strength and axial strain of the sample with crack inclination angle are drawn, as shown in Figure 4. As can be seen from the figure, the compressive strength and axial strain of the specimen gradually decreased with the increase in the prefabricated crack inclination angle. The compressive strength and axial strain of the complete

(a) (b)

Figure 3: Crack morphology after specimen failure: (a) crack morphology after failure of the cylindrical specimen; (b) crack morphology after failure of the disc specimen.

Table 2: Axial strain and compressive strength of cylindrical specimens under uniaxial compression.

Number of sets of sample	Crack angle (°)	Mean axial strain (%)	Average uniaxial compressive strength (MPa)
1	Complete	1.41	70.12
2	0	1.32	46.58
3	15	1.22	44.87
4	30	1.06	42.62
5	45	0.94	35.44
6	60	0.81	30.21
7	75	0.62	25.86
8	90	0.52	18.99

specimen were 70.12 MPa and 1.41%, respectively. The compressive strength and axial strain of the specimen with prefabricated crack 90° reached the minimum, 18.99 MPa and 0.52%, respectively. On the whole, the stress-strain curve of the sample can be divided into four stages: compaction, elasticity, plasticity, and residual deformation.

By observing the crack morphology of each group of samples after failure, it can be seen that the failure morphology of samples is different. After the complete specimen was destroyed, irregular longitudinal cracks were formed, accompanied by multiple microcracks, and the volume of the specimen expanded. For the prefabricated crack sample with a dip angle of 0°, the crack initiation location occurs at the upper tip of the crack, and it is a tension wing crack and parallel to the loading direction. For the prefabricated crack sample with an inclination angle of 15°, there are tension wing cracks on the upper and lower tips of the crack, and a crack running through the side of the crack is formed. The prefabricated crack sample with an inclination angle of 30° has a concentrated stress at the crack tip, and the crack propagation occurs at both ends of the specimen and finally extends to the upper and lower ends of the specimen. When the inclination angle was 45°, the tensile wing and the composite wing cracks were generated at the upper tip of the crack and finally extended to the upper part of the specimen, and the secondary cracks were generated at the lower tip of the crack and finally extended to the lower part of the specimen. The prefabricated crack sample with an inclination angle of 60° showed new cracks which extended to the end of the sample. In the sample with a prefabricated crack angle of 75°, the same new crack appeared as in the sample with a prefabricated crack angle of 60°, and the crack propagated in the middle of the crack and extended to the end face of the sample. The crack initiation and propagation direction of the prefabricated specimen with an inclination angle of 90° tend to be parallel to the loading direction of the specimen, and shear slip failure and tension crack occur in the specimen.

According to the failure mode of the cylinder sample, it can be seen that the crack initiation angle increases gradually with the increase in the prefabricated crack angle. At the initial stage of the test, stress concentration occurs at the crack tip, and the crack tip begins to expand and form a wing crack. With the increase in load, new stress concentration occurs, which leads to secondary crack and antiwing crack. When the load reaches a certain value, cracks are connected and fracture failure occurs. On the whole, with the increase in the prefabricated crack angle, the failure of the specimen changes from shear slip failure to split shear failure of the penetrating rock mass.

3.2. Experimental Results of the Disc-Shaped Sample. For the disk-shaped sample, the peak load and peak displacement of each sample were obtained through uniaxial compression, as shown in Table 3. According to Table 3, the variation rule of peak load and peak displacement of samples with crack angle was drawn, as shown in Figure 5. As can be seen from the figure, the peak load of the complete specimen is 9.26 kN, which is at least twice the peak load of the prefabricated cracked specimen. The peak displacement of 0.245 mm is also the largest. The prefabricated crack specimens with various dip angles fell rapidly after the load reached the peak and the small displacement resulted in the failure of the specimen. With the increase in the prefabricated crack dip angle, the peak load of the sample first decreases and then increases. When the crack dip angle is 30°, the peak load is the smallest, which is 2.32 kN. The peak displacement of the sample drops sharply at first and then slowly declines

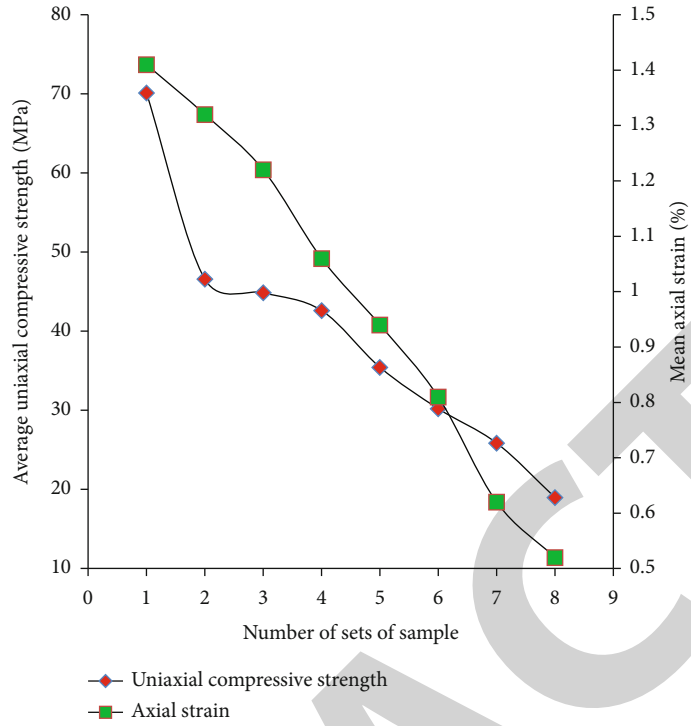

Figure 4: Variation of compressive strength and axial strain with crack angle of the cylindrical specimen.

Table 3: Peak load and peak displacement of the disc specimen under uniaxial compression.

Number of sets of sample	Crack angle (°)	Mean peak displacement (mm)	Average peak load (kN)
1	Complete	0.245	9.26
2	0	0.174	4.62
3	15	0.163	3.49
4	30	0.152	2.32
5	45	0.147	3.95
6	60	0.155	4.31
7	75	0.143	4.88
8	90	0.132	5.12

but suddenly increases when the crack dip angle is 60°, which is mainly due to the change of the internal stress structure of the specimen caused by the increase in the crack dip angle. Therefore, the failure mode of the specimen changes, and the failure location changes from the prefabricated crack tip to the middle.

By observing the crack morphology of each group of disk samples after failure, it can be seen that the main crack of the complete sample runs through the whole disk, and the formation of the crack is related to the tensile action of the specimen. For the specimen with prefabricated crack 0°, the crack initiation occurred at the upper tip, which was a tension wing crack. For the specimen with a prefabricated crack of 15°, the prefabricated crack initiation position was at the upper and lower tips, and tension wing cracks were produced, accompanied by a large number of secondary cracks. For the specimen with a prefabricated crack of 30°, the stress concentration at the tip of the prefabricated crack leads to the failure of the specimen, and the tensile and shear wing cracks of the new crack extend to the upper and lower end faces of the specimen. The stress concentration at the crack tip was enhanced for the specimen with a prefabricated crack of 45°, while the tensile wing cracks and the tension-shear composite wing cracks generated at both ends of the prefabricated crack continued to extend to the upper and lower ends of the specimen. For the specimen with a prefabricated crack of 60°, the shear wing crack and tension wing crack were mainly generated at both ends of the prefabricated crack and extended to the upper and lower ends of the specimen, and the main crack was in the shape of an arc. For the specimen with a prefabricated crack of 75°, tensile and shear cracks and tensile cracks were generated in the middle of the prefabricated crack and extended to the upper and lower end faces of the specimen, and the tensile cracks were the main crack initiation. The prefabricated specimen with a crack of 90° produced a tensile crack in the middle of the prefabricated crack after loading, and the direction of the crack after initiation tended to be parallel to that of the loading direction, similar to that of the complete specimen.

According to the failure mode of the disk sample, it is obvious that the crack initiation angle increases gradually with the increase in the prefabricated crack inclination angle, but when the inclination angle exceeds 75°, the crack initiation location occurs in the middle of the crack. The failure modes of disc-shaped specimens under cracks with different dip angles indicate that the main reason for the failure of specimens lies in the connection and extension of cracks.

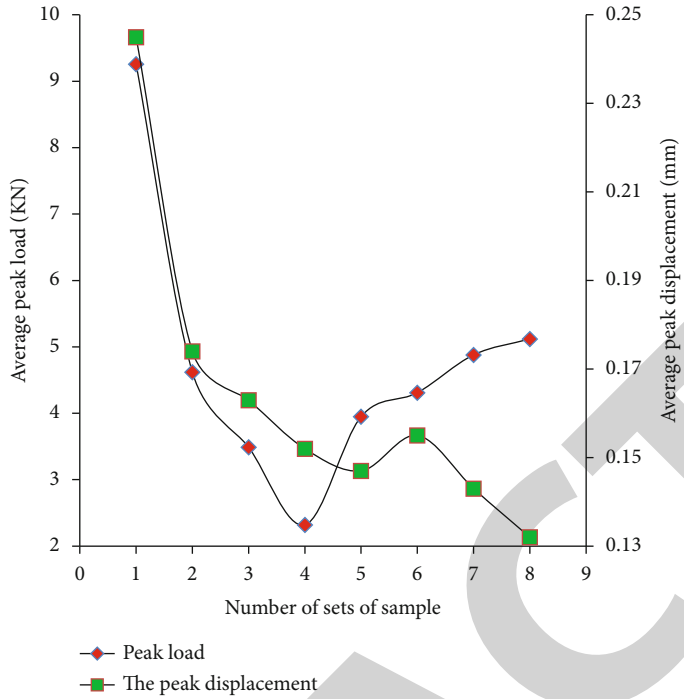

Figure 5: The variation of peak load and peak displacement of the disc-shaped sample with crack angle.

With the increase in the prefabricated crack angle, the crack initiation position gradually transitioned from the crack tip to the middle of the crack. For the specimens with crack inclination angles of 60°, 75°, and 90°, the crack initiation position all occurred at the crack center. This is obviously different from the crack propagation law of the cylinder uniaxial compression test. In general, with the increase in the prefabricated crack angle, the fracture modes of the specimen change greatly, which is obviously different from the fracture characteristics of the complete disk specimen.

4. Conclusion

The propagation of cracks in rock mass has always threatened the safety of geotechnical engineering construction and the stability of rock mass. In this paper, uniaxial compression tests were carried out on cylindrical and disk-shaped specimens with different prefabricated crack dip angles and different shapes. The mechanical properties of specimens with different prefabricated crack dip angles and different shapes were studied. The crack propagation law during the fracture process of specimens was analyzed, and the influence mechanism of crack dip angle and sample shape on crack propagation was revealed. The following are the main research achievements of this paper:

(1) Uniaxial compression of cylindrical and disc-shaped granite samples was carried out using RMT-150C rock mechanics testing machine. The stress-strain curves of the samples can be divided into four stages: compaction, elasticity, plasticity, and residual deformation. The compressive strength and peak stress of the complete samples are higher than those of the cracked specimens

(2) For the cylindrical specimen, the compressive strength and axial strain decrease gradually with the increase in the prefabricated crack inclination angle. The crack initiation positions of all specimens with cracks occur at the tip, and the crack initiation angles increase with the increase in the prefabricated crack inclination angle. With the increase in crack inclination angle, tip crack expands to wing crack, and new stress concentration in the specimen forms secondary crack and antiwing crack. Finally, crack coalescence leads to specimen failure. On the whole, with the increase in prefabricated crack angle, the failure of the specimen changes from shear slip failure to split shear failure of the penetrating rock mass

(3) For the disk sample, the peak load of the complete specimen is much larger than that of the specimen with prefabricated crack, and the specimen with prefabricated crack immediately fails after reaching the peak load. The peak load of specimens decreases first and then increases with the increase in the prefabricated crack angle. The peak load of specimens with a crack angle of 30° is the smallest, which is 2.32 kN. Crack angle increases as the prefabricated crack angle increases gradually; the crack position enters the middle through the tip with an angle of more than 75°, which changes the fracture mode of the sample and completes the disc fracture and the characteristics of the sample. The main reason for the damage of the disc sample is the crack penetration and propagation. The crack initiation positions of

the specimens with crack dip angles of 60°, 75°, and 90° all occurred at the crack center, which was obviously different from the crack propagation law of the cylinder specimens with crack dip angles of the same

(4) Under the condition of consistent prefabricated crack angle, the test results of rock samples with sampling depth of 50 m, 100 m, 150 m, and 200 m are similar, and the sampling depth basically has no effect on the law of rock crack propagation

Data Availability

The figures and tables used to support the findings of this study are included in the article.

Conflicts of Interest

The authors declare that they have no conflicts of interest.

Acknowledgments

The authors would like to show sincere thanks to those techniques who have contributed to this research.

References

[1] B. Haimson and C. Chang, "A new true triaxial cell for testing mechanical properties of rock, and its use to determine rock strength and deformability of Westerly granite," *International Journal of Rock Mechanics and Mining Sciences*, vol. 37, no. 1-2, pp. 285–296, 2000.

[2] T. A. K. A. S. H. I. Satoh, O. S. A. M. U. Nishizawa, and K. Kusunose, "Fault development in Oshima granite under triaxial compression inferred from hypocenter distribution and focal mechanism of acoustic emission," *Science Report Tohoku University*, vol. 5, no. 33, pp. 241–250, 1990.

[3] J. He, C. Lin, X. Li, and X. Wan, "Experimental investigation of crack extension patterns in hydraulic fracturing with shale, sandstone and granite cores," *Energies*, vol. 9, no. 12, p. 1018, 2016.

[4] X. Zhou, M. Yi, J. Zhou, H. Cheng, and F. Berto, "Experimental study on the progressive failure of double-flawed granite samples subjected to impact loads," *Fatigue & Fracture of Engineering Materials & Structures*, vol. 45, no. 3, pp. 653–670, 2022.

[5] M. H. B. Nasseri, B. S. A. Tatone, G. Grasselli, and R. P. Young, "Fracture toughness and fracture roughness interrelationship in thermally treated westerly granite," *Pure and Applied Geophysics*, vol. 166, no. 5-7, pp. 801–822, 2009.

[6] Y. Zhou, D. Zhao, Q. Tang, and M. Wang, "Experimental and numerical investigation of the fatigue behaviour and crack evolution mechanism of granite under ultra-high-frequency loading," *Royal Society Open Science*, vol. 7, no. 4, p. 200091, 2020.

[7] G. Walton, L. R. Alejano, J. Arzua, and T. Markley, "Crack damage parameters and dilatancy of artificially jointed granite samples under triaxial compression," *Rock Mechanics and Rock Engineering*, vol. 51, no. 6, pp. 1637–1656, 2018.

[8] H. Kawakata, A. Cho, T. Yanagidani, and M. Shimada, "The observations of faulting in westerly granite under triaxial compression by X-ray CT scan," *International Journal of Rock Mechanics and Mining Sciences*, vol. 34, no. 3-4, pp. 151.e1–151.e12, 1997.

[9] M. H. B. Nasseri, A. Schubnel, and R. P. Young, "Coupled evolutions of fracture toughness and elastic wave velocities at high crack density in thermally treated Westerly granite," *International Journal of Rock Mechanics and Mining Sciences*, vol. 44, no. 4, pp. 601–616, 2007.

[10] I. A. Panteleev, "Analysis of the seismic moment tensor of acoustic emission: granite fracture micromechanisms during three-point bending," *Acoustical Physics*, vol. 66, no. 6, pp. 653–665, 2020.

[11] R. H. C. Wong, C. A. Tang, K. T. Chau, and P. Lin, "Splitting failure in brittle rocks containing pre-existing flaws under uniaxial compression," *Engineering Fracture Mechanics*, vol. 69, no. 17, pp. 1853–1871, 2002.

[12] J. W. Zhou, W. Y. Xu, and X. G. Yang, "A microcrack damage model for brittle rocks under uniaxial compression," *Mechanics Research Communications*, vol. 37, no. 4, pp. 399–405, 2010.

[13] L. Weng, X. Li, A. Taheri, Q. Wu, and X. Xie, "Fracture evolution around a cavity in brittle rock under uniaxial compression and coupled static–dynamic loads," *Rock Mechanics and Rock Engineering*, vol. 51, no. 2, pp. 531–545, 2018.

[14] R. H. Cao, P. Cao, X. Fan, X. Xiong, and H. Lin, "An experimental and numerical study on mechanical behavior of ubiquitous-joint brittle rock-like specimens under uniaxial compression," *Rock Mechanics and Rock Engineering*, vol. 49, no. 11, pp. 4319–4338, 2016.

[15] W. A. N. G. Linjun, Z. H. A. N. G. Bo, Q. I. A. N. Zhikuan, L. E. Qiaoli, and H. O. N. G. Jingjing, "Experimental investigation of the acoustics emission characteristics of two types of brittle rocks under uniaxial compression," *Journal of Engineering Geology*, vol. 27, no. 4, pp. 699–705, 2019.

[16] W. Yang, G. Li, P. G. Ranjith, and L. Fang, "An experimental study of mechanical behavior of brittle rock-like specimens with multi-non-persistent joints under uniaxial compression and damage analysis," *International Journal of Damage Mechanics*, vol. 28, no. 10, pp. 1490–1522, 2019.

[17] Q. Zhu, D. Li, Z. Han, P. Xiao, and B. Li, "Failure characteristics of brittle rock containing two rectangular holes under uniaxial compression and coupled static-dynamic loads," *Acta Geotechnica*, vol. 17, no. 1, pp. 131–152, 2022.

[18] E. G. Bombolakis, "Study of the brittle fracture process under uniaxial compression," *Tectonophysics*, vol. 18, no. 3-4, pp. 231–248, 1973.